



Uptake of acid blue 113 dye from aqueous solution by sludge/floc nanoparticles in electrocoagulation process

Rojan Akhbarati^a, Elham Keshmirizadeh^{a,*}, Hamid Modarress^b

^aDepartment of Chemistry, Karaj Branch, Islamic Azad University, Karaj, Iran, P.O. Box: 31485-313, Tel. +98-263-4182318, email: rojan_akhbarati@yahoo.com (R. Akhbarati), Tel. +98-263-4182305, Fax +98-263-4418156, email: keshmiri@kiaau.ac.ir (E. Keshmirizadeh),

^bDepartment of Chemical Engineering, Amir-Kabir University of Technology, No. 424, Hafez Avenue, P.O. Box: 15875-4413, Tehran, Iran, Tel. +98-216-454 3176, Fax +98-216-6405847, email: hmodares@aut.ac.ir

Received 27 November 2016; 4 August 2017

ABSTRACT

Electrocoagulation (EC) process has been used for uptake of acid blue 113 (AB113) dye as a hazardous pollutant. The operating parameters of EC process by application of iron(anode)/aluminum (cathode) as the electrodes were optimized by considering the effect of initial dye concentration, initial pH, current density, electrolyte concentration, water reclamation yield, type of current (direct current (DC) and square pulse current (SPC)), electrical energy and specific electrical energy consumption (SEEC). The results indicated that SPC was found distinctive to DC for the AB113 dye removal by EC based on significantly high values of dye uptake (%), water reclamation yield and energy economization. The dried sludge/floc was characterized by scanning electron microscopy (SEM), energy dispersive analysis of X-ray (EDAX), X-ray diffraction (XRD) and Fourier transform infrared spectroscopy (FTIR). The dried sludge/floc was in the form of nano pseudo sphere of iron and aluminum hydroxide particles. The dye adsorption results were treated by several adsorption isotherms equations and it was found that the Sips isotherm equation indicated the best fit to the obtained results. Also among the rate equations, it was found that the pseudo-second-order rate equation properly expressed the rate of the dye adsorption.

Keywords: Acid blue113; Electrocoagulation; Sludge/floc nanoparticles; Square pulse current

1. Introduction

The discharges of many industries such as textile, plastic and cosmetics are highly polluted and colored due to presence of toxic dyestuff [1–4]. The water soluble acid blue 113 dye as used or produced in various industries can be classified as an anionic types of dye which has di-azo chromophore groups linked to aromatic rings [5]. Because of a large volume of the industrial dye effluents, such as acid blue113 dye, their removal from environment is one of the basic problems [6]. The electrocoagulation (EC) process is an efficient method for removal of pollutants and hazardous materials [7–17]. In the EC operation various chemical conversions and physical operations are performed, namely during electrolysis,

metallic electrodes such as Fe (anode)/Al (cathode) are dissolved in the electrolyte solutions and based on pH many ionic species of a metal (M) such as $M(OH)^{2+}$, $M(OH)_2^+$ and insoluble precipitates such as $M(OH)_3$ are formed; which can coagulate and adsorbed dye to become a floated floc or a sediment of precipitant [4,17]. The principal reactions occurring at the anode are water electrolysis and oxidation or dissolution of the electrode whereas at the cathode the reduction reaction occurs. The hydroxide ions can enhance the pH of the aqueous electrolyte solution and the amorphous and gelatinous solid, $M(OH)_3$ which appears as sweep floc has a significant surface area and can be utilized as a good adsorbent for adsorption of dissolved organic molecules [8]. Subsequently these sticky and gelatinous coagulums are effective for trapping the pollutants such as dye particles and are readily separated from the aqueous solution by

*Corresponding author.

precipitation or floating on the solution surface [18]. Based on the Faraday's law, the theoretical amounts of electrode metal dissolution (m) (and also hydroxide ions) produced at a particular time in the EC reactor can be calculated by using the following equation [9,19–21]:

$$m = \frac{ItM}{zF} \quad (1)$$

where m (g) is the mass loss of the anode at the end of EC operation time, M (g/g mole) is the molecular weight of metal or hydroxide ion (55.85 for iron, 26.98 for Aluminium and 17 for hydroxide), I electric current (amper), F is the Faraday's constant 96486 C/mol and z is the number of transferred electrons in the reaction (2 for iron, 3 for Aluminium and 1 for hydroxide). At very high dosages of hydroxide coagulation the precipitation of coagulants may occur [22].

In this research the important operating conditions such as initial pH, initial dye concentration, current density and dose of electrolyte for the removal of AB113 dye were optimized by imposing direct and in square pulse currents. Also for improvement of the dye removal efficiency, the energy economization, economic analysis and also the enhancement of water reclamation yield were investigated. The electrocoagulated sludge/floc was characterized by SEM, FTIR, XRD and EDAX analysis. The adsorption results were treated by using the adsorption isotherm equations and adsorption rate equation.

2. Experimental

2.1. Material

Acid blue 113 dye ($C_{32}H_{21}N_5Na_2O_6S_2$, MW 681.65 g/g-mol, with a maximum absorbance wavelength at 566 nm) was supplied by Alvan-sabet rang company (Iran) and used without further purification. The molecular structure of the acid blue 113 dye (AB113) is shown in Fig. 1. All other reagents such as HCl, NaOH and NaCl were of analytical grade and were obtained from Sigma-Aldrich (Germany).

2.2. Experimental setup

Batch electrochemical experiments were done in a one liter Plexiglas electrochemical cell equipped with Fe (anode) and Al (cathode) electrodes. The electrode plates were provided by Nano-Pushesh Felez Company (Iran), with the submerged surface area of 49 cm² (7 cm × 7 cm) and 2 mm

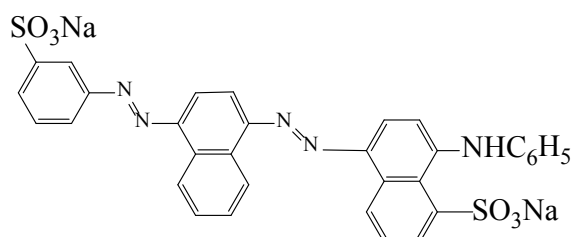


Fig. 1. Molecular structure of acid blue 113 (AB113).

thickness. The electrodes distance was fixed at 2.5 cm. The initial working volume of the AB113 dye aqueous solution was 700 mL. Direct and square pulse power supply, and the device for measuring and regulating the reactor voltage (220 V input/0–30 V output) and amperage (0–4 A) were obtained from Nano-Pushesh Felez Company (Iran). The applied amperage in all experiments (at) was 0.68 A. Mother dye aqueous solution (1000 mg/L) was prepared by adding an appropriate amount of AB113 dye in a certain volume of de-ionized water. The adsorption isotherms were studied for the initial dye concentrations varying from 20 to 500 mg/L. But the adsorption rates were evaluated by using 500 mg/L as the initial dye concentration. NaCl was used as a supporting electrolyte and the conductivity of the dye solution was adjusted at 1.7 mS/cm. The initial pH of the dye solution was varied by adding NaOH (0.1 M) and HCl (0.1 M) solutions. The stirring speed of solution was set at 100 rpm. The supernatant was analyzed every 1 min. Schematic diagram of electrocoagulation reactor is shown in Fig. 2. The sludge/floc sample was separately filtered from supernatant and was set to dry for 72 h at 65 in an oven before characterization by SEM, EDAX and FTIR. Each experiment was repeated twice and the results showed that the reproducibility of the obtained results was less than 4%.

2.3. Method

During the EC process the conductivity was measured based on the 2510-B method [23] by making use of a conductometer (Hach-Longe, model: HQ30D, Germany), and the pH was measured with a Metrohm pH meter (model 827, Switzerland). The turbidity of the solution before and after EC process was determined based on the 2130-B [23] (nephelometric method) by using the turbiditymeter (Hach-Longe, model: 2100N, Germany). The scanning electron microscopy (SEM) was carried out on model EM3200, KYKY Canada. The FTIR absorption spectrum was performed by applying KBr discs on a Perkin-Elmer/USA spectrometer in the range 4000–4500 cm⁻¹. The color and chemical oxygen demand (COD) measurements [24] of the samples were based on the standard method [23], by using a double beam and auto scan UV-Vis spectrophotometer (Hach-Longe, model: DR2800, Germany). A calibration curve was prepared by plotting the variation of dye absorbance (at

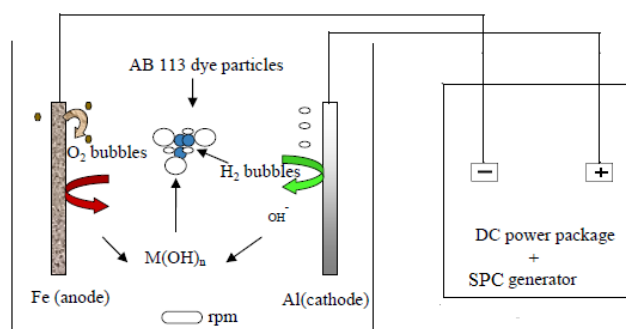


Fig. 2. Schematic diagram of electrocoagulation (EC) apparatus, DC: direct current; SPC: square pulse current.

maximum wavelength of 566 nm) vs dye concentration. The dye removal efficiency or uptake percentage was calculated by the following equation:

$$\text{Uptake}\% = 100 \times \left(1 - \frac{C_e}{C_0} \right) \quad (2)$$

where C_0 and C_e (mg/L) are the initial and final dye concentration in the EC process respectively.

The electrical energy was calculated by using the following equation [7]:

$$E = \frac{\varepsilon \cdot i \cdot t}{V} \quad (3)$$

where E (kWh/ m³) is the electrical energy for treatment of 1 m³ of the AB113 dye, (*volt*) is the voltage, i (A) is the current, t (h) is the equilibrium EC time and V (m³) is the initial volume of AB113 dye aqueous solution.

The water reclamation yield (WRY) is expressed as:

$$\text{water reclamation yield (WRY)} = \frac{\text{volume of clear supernatant after the dye removal}}{\text{volume of the solution before the dye removal}} \quad (4)$$

where the “water reclamation yield” is expressed in m³ of clear supernatant after removal/m³ of the solution before removal if the turbidity of clear supernatant after the dye removal was 4NTU [23]. As it is shown in Fig. 2 after EC process, a dewatered sludge and also densely lighted flocs based on their densities are formed at the bottom and top of the surface of the reactor, respectively [7].

3. Results and discussion

3.1. Influence of initial pH

The EC process is effectively dependent on the pH of the aqueous dye solution [25]. It is reported that when the initial pH is in the range of 4 to 8 all the metal (M) cations at the anode, form polymeric moieties $M_{13}O_4(OH)_{24}^{7+}$ and precipitate as $M(OH)_3$ which can effectively destroy the pollutants [1,19]. In Fig. 3 the effect of initial pH on the AB113 dye uptake % is demonstrated and it is seen that for the initial pH increase from 1 to 5, the final pH increases from 2.5 to 7, and the dye uptake % approaches a maximum value of 99%. By increasing the initial pH from 5 to 9 the dye uptake % decreases from 99% to 78% where the final pH is more than 11.

The decreases of uptake % at a pH less than 5 and higher than 7, has been reported by researchers and has been ascribed to ionic presence of species or it might be due to presence of other soluble species at low and high pH [1,20]. The high uptake % of AB113 dye at pH 5 can be attributed to the production of insoluble metal hydroxides in the solution. Fig. 3 represents that the AB113 dye removal process is more efficient at the initial pH 5. A similar trend for pH variation demonstrated by other researcher for Fe/Al electrodes [26].

3.2. Influence of current density

The current density (CD) is the determining factor in controlling the rate of EC operation because it regulates the

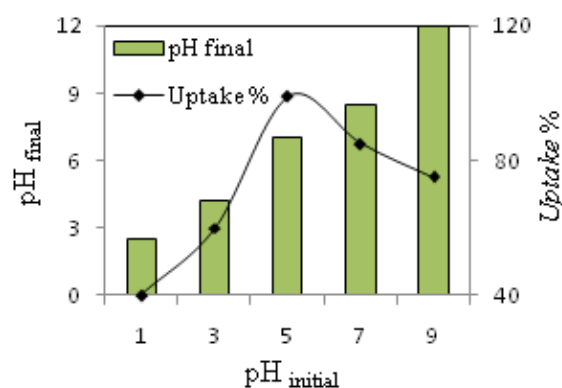


Fig. 3. Effect of initial and final pH on the AB113 uptake % (at the optimum condition; initial dye concentration 500 mg/L, CD 70 A/m², conductivity 1.7 mS/cm, equilibrium time 12 min).

amount of coagulant, the rate and also the size of bubble production [19]. The bubble size decreases by increasing CD, and this phenomenon is very helpful in the separation stage [21]. Based on Faraday's law [Eq. (1)] the amounts of metal hydroxide ions produced at a certain time during EC process is related to the current density (CD) according to the following equation [7]:

$$CD = \frac{I}{2A} \quad (5)$$

where I (A) is current or amperage and A (m²) is the surface area of the electrode. To study the effect of CD in the variation range of 20–120 (A/m²) on the uptake % of the dye, a series of experiments were performed at constant initial dye concentrations (for example 500 mg/L), to obtain the optimum current required to accomplish a low cost and successful dye removal. Fig. 4 demonstrates the variation of uptake % vs. CD. As illustrated in this figure, for an initial dye concentration of 500 mg/L, the CD is 70 A/m² and after 12 min of electrolysis and at the initial pH 5, the uptake % of the dye reaches a value of 99%. However by increasing the CD up to 120 A/m² the uptake % remained constant. Furthermore, it can be shown that the uptake % of the dye decreases significantly upon the CD decrease. These results represent an enhancement compared with previously reported results [16,27]. It should be noted that most researchers introduced an optimum CD greater than 100 or 200 A/m² for the hybrid Fe/Al electrode or other kind of electrodes. But in this research optimum CD was 70 A/m² for an uptake % of 99% [27,28].

3.3. Effect of electrolytes dose

The supporting electrolyte concentration is a predominant factor on the dye treatment process by EC. The solution conductivity increases by the addition of NaCl. Also NaCl hinders the polarization or anode passivity (IR-drop) and the chloride ion has catalytic role on dissolution of the electrodes [29]. For iron as the anode, the presence of chloride ion causes the following reaction to occur in the solution bulk [Eqs. (6)–(9)] and in the anode [Eqs. (10)–(12)] [30]:

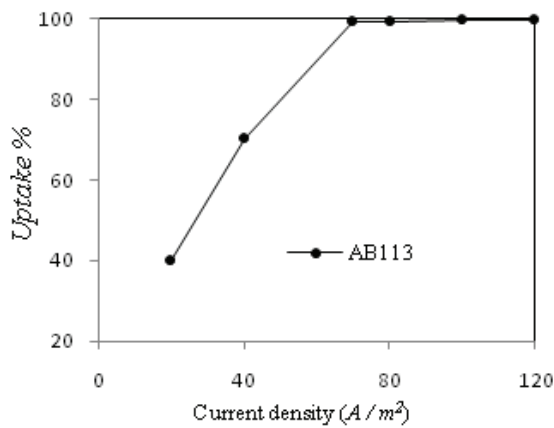


Fig. 4. Effect of current density on the uptake % of AB113 dye (at the optimum condition; initial dye concentration 500 mg/L, initial pH 5, conductivity 1.7 mS/cm, equilibrium time 12 min).

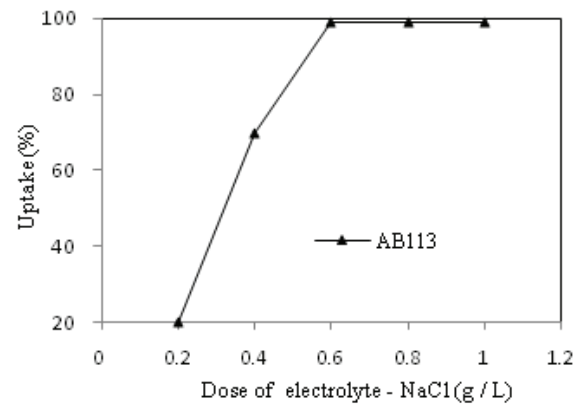
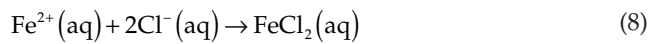
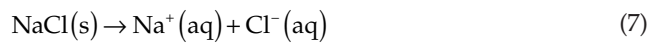
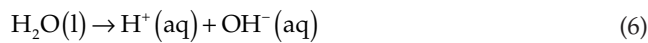
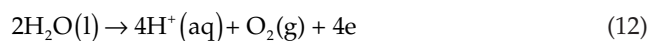


Fig. 5. Effect of electrolyte (NaCl) concentration on the uptake percentage of AB113 dye (at the optimum condition; initial dye concentration 500 mg/L, initial pH 5, current density 70 A/m², equilibrium time 12 min).



and then for formation of $\text{Fe}(\text{OH})_3$ flocs at $6 < \text{pH} < 9$ [31–33]:



The generated due to dismutation reaction at $\text{pH} > 4$ [Eqs. (13), (14)] [12,15]:



The produced O_2 , ClO^- and Cl_2 can act as oxidizing reagents for enhancing the dye removal [12]. Based on the solution pH, the gelatinous suspension include monomeric or polymeric complexes of iron hydroxide (such as: $\text{Fe}(\text{OH})_3$, $\text{Fe}(\text{OH})_4^-$, $\text{Fe}(\text{H}_2\text{O})_3(\text{OH})_3$, $\text{Fe}_2(\text{H}_2\text{O})_8(\text{OH})_2^{4+}$) which remain in the aqueous solution to remove the dye molecules by electrostatic attraction, coagulation and then settling [32–34].

However the cathodic reaction is:



For different concentrations of NaCl, at the initial AB113 dye concentration of 500 mg/L and pH 5 after 12 min of EC operation the values of uptake (%) are presented in Fig. 5. As expected at low chloride ions concentration, the uptake (%) is less than 60% which is due to the partial Fe anode polarization or passivity, which prevents Fe^{2+} and production. Therefore the coagulation and AB113 dye removal is hindered. As shown in Fig. 5 by addition of chloride ions up to 0.6 g/L the uptake (%) increases to 99%, then remains constant. These results are in agreement with the previous studies [12,14].

3.4. Effect of initial dye concentration on the EC time

The AB113 dye solutions with different initial concentrations for 20–500 mg/L were treated by EC process at optimum condition of, $\text{pH} = 5$, $\text{CD} = 70 \text{ A/m}^2$ and 12 min equilibrium time. Variations of AB113 uptake (%) vs. EC time at different initial dye concentrations are represented in Fig. 6. As the results in Fig. 6, indicate, at the beginning the uptake (%) sharply increases, then approaches to a limit and remains constant. It can be seen that the most of initial dye is removed within the first 7 min of EC time and then uptake (%) is neglect after 12 min. Also Fig. 6 indicates that the uptake (%) decreased with increasing in the initial dye concentration. This can be interpreted by considering the fact that at this fixed experimental conditions the amount of coagulant production is also fixed. Therefore, the ratio of coagulant to the initial dye concentration or uptake (%) indicates a decreasing trend with increasing. A similar pattern has been reported by other researchers [25,27].

3.5. Type of current pattern, direct current (DC) and square pulse current (SPC)

In this investigation the effect of two different types of circuit in the EC process have been investigated to obtain a specific and economical AB113 dye removal conditions. In the EC process at first some coagulants,

flocs and gelatinous metal oxides are formed around the electrodes due to oxidation of sacrificial anode (Fe) and then afterward the undesired polarization and passivity phenomena occurs [35,36]. In order to prevent the polarization, square pulse current (SPC) was applied [16,37]. Fig. 7 shows that the SPC pattern as compared with direct current (DC). In the DC pattern the electrodes

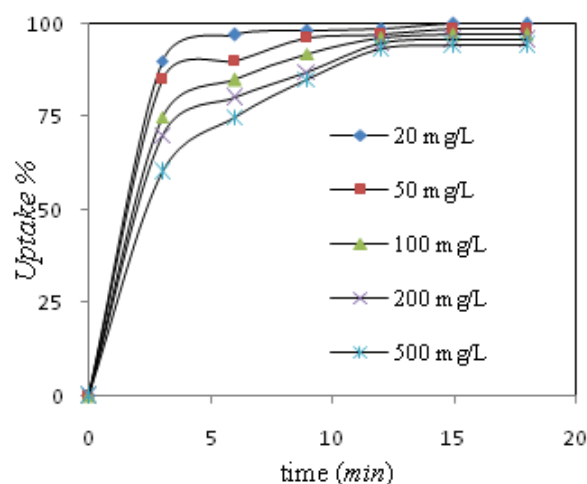


Fig. 6. Influence of initial AB113 dye concentration on its uptake % (at the optimum condition; CD 70 A/m², initial pH 5, conductivity 1.7 mS/cm, equilibrium time 12 min).

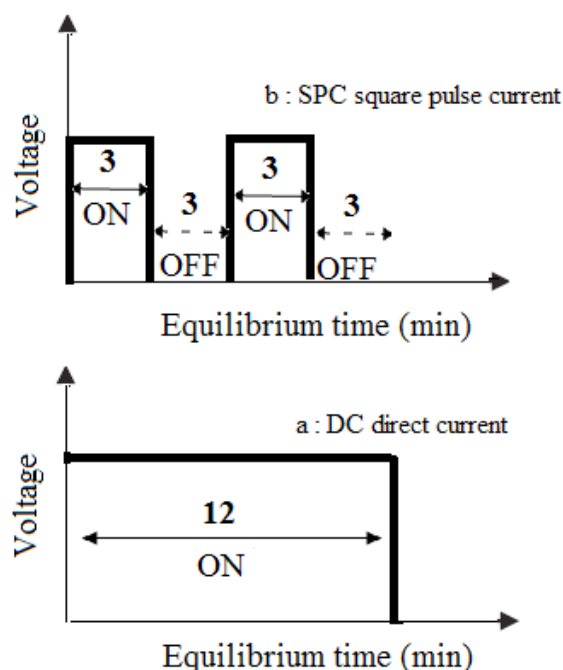


Fig. 7. Schematic pattern for (a): direct current (DC), the electrodes (Fe and Al) are operating continuously for 12 min at maximum voltage afterward the voltage is decayed to zero at the end of EC process, and (b): square pulse current (SPC), the electrodes (Fe and Al) are operating for 3 min at maximum voltage afterward the voltage is decayed to zero for 3 min and these intervals are repeated in the course of EC process.

(Fe and Al) are working at the maximum applied voltage continuously for 12 min (equilibrium EC time). Then the voltage is decayed to zero at the end of EC process whereas in SPC two electrodes are working for 3 min of the pulse duration, at the maximum applied voltage (12–20 V) and then the voltage is decayed to zero for 3 min and this intervals is repeated in the course of EC process. Actually the occurrence of this on/off of the applied voltage, in the course of EC process, not only can eliminate the fouling of sludge around the electrodes, it would help economization of electrical energy [Eq. (3)]. Table 1 reports the effect of the successive pulse duration time length for SPC (3 min on/3 min off). Also in this Table the uptake %, electrical energy and water reclamation yield as calculated by Eq. (4), are compared with the results obtained by DC pattern. Based on these results the dye removal efficiency or uptake % and water reclamation yield are higher in using SPC pattern (0.95 m³ of clear supernatant after removal/m³ of the solution before removal) than DC (0.7 m³ of clear supernatant after removal/m³ of the solution before removal) also electrical energy in SPC 1.2 kWh/m³ of the solution before removal is lower than DC (3.7 kWh/m³ of the solution before removal). In Table 1 electrical energy is calculated and represented for different types of SPC current as well as DC current, the results represented that the electricity cost of 0.044 €/m³ (at 98% uptake and WRY 0.7 m³/m³) was reduced to 0.014 €/m³ (at 99.66% uptake and WRY 0.95 m³/m³) with the changing current mode from DC to SPC based on the electricity cost (see Table 2) of 0.012 €/kWh (Iranian marketing price at Jun. 2017). Phalakornkule et al. [2] found that the electrical energy of the EC process for removal of Reactive Blue 140 and Direct Red 23 dye solutions were 1.42 and 0.69 kWh/m³, respectively. Therefore as expected the results of COD measurements [24] in SPC electro coagulation for AB113 dye indicated that % COD removal efficiency in the optimized condition is significant (as much as 94%).

3.5.1. Economic analysis

In any electrocoagulation process the total cost estimation is investigated due to electrical energy requisition, operating cost and fixed cost. The total cost is expressed as Eq. (16):

$$\text{Total}_{\text{cost}} = \text{Electricity}_{\text{cost}} + \text{Purchased}_{\text{cost}} + \text{Labor}_{\text{cost}} + \text{Sludge disposal}_{\text{cost}} + \text{Fixed}_{\text{cost}} \quad (16)$$

where the operating cost includes cost of electrode sheet and chemical reagent (purchased cost), sludge discarding and also worker or labor as well as the fixed cost, such as cost of EC tank reactor, power supply and also the cost of maintenance and repair services. In Table 2 the prices of each term and item in Eq. (16) in the Iranian market given for Jun 2017 were represented.

The current efficiency, Δ (%), or Faradic yield percent which can be a pitting corrosion criteria [38–40] is defined as Eq. (17) [4,41]:

$$\Delta(\%) = \frac{\text{Electrode weight loss}_{\text{Exp.}}}{\text{Electrode weight loss}_{\text{Theo.}}} \times 100 \quad (17)$$

Table 1

Comparison the effect of square pulse current (SPC) and direct current (DC) on uptake % of AB113 dye by EC process (at the optimum condition; initial pH 5, initial dye concentration 500 mg/L, conductivity 1.7 mS/cm, I 0.68 A, CD 70 A/m², volume of wastewater 700 mL)

Type of current	Time off	Time on	Dye residual concentration	Uptake Eq. (2)	Electrical energy Eq. (3)	Electricity cost	SEEC Eq. (18)	Water reclamation yield, Eq. (4)
SPC	(min)	(min)	(mg/L)	(%)	(kWh/m ³ of the solution)	€/m ³	kWh/(kg Fe)	(m ³ /m ³ of the solution)
	1	1	5	99.00	0.021	0.021	0.16	0.80
	2	2	5	99.00	1.8	0.016	0.12	0.90
	1	2	4	99.20	1.4	0.024	0.15	0.85
	*3	3	1.67	99.66	2.0	0.014	0.10	0.95
**DC	-	12	5	98.0	3.7	0.044	0.18	0.7

****: Optimum condition for SPC, **: Optimum condition for DC.

Table 2

Economic cost estimation used in the total cost calculation for electrocoagulation process

Item description	Cost quote unit	Cost, € (Jun., 2017) ^a
Electricity cost (Eq. (3))	kWh	0.012
Purchased cost		
Sheet metals for electrode (Fe)	Kg	0.04
Sheet metals for electrode (Al)	Kg	0.32
Chemical reagent		
Sodium chloride as electrolyte	Kg	0.4
Hydrochloric acid for pH adjustment	Lit	0.6
Sodium hydroxide for pH adjustment	Lit	0.7
Labour cost	m ³	0.1
Sludge disposal cost	Kg	0.01
Fixed cost (equipment, installation & maintenance)		
Electrocoagulation tank reactor (5 m ³)	# ^b	200
Electrical DC power supply	# ^b	300
Maintenance and accessories	- ^c	0.005

a: Iranian Marketing Reporter; b: for a unit; c: not predictable.

Δ (%), was calculated separately for anode (Fe) and cathode (Al) electrodes. For experimental electrode weight loss, each electrode weighted before and after the electrocoagulation process so the amount of experimental electrode weight loss was reported, as an example for the optimum SPC current conditions represented in Table 1 (SPC (On – 3 min), (Off – 3 min), I = 0.68 A, EC time = 6 min), the real anode and cathode weight loss are 0.11 kg/m³ and 0.035 kg/m³ respectively. However the theoretical anode and cathode weight loss using Eq. (1) at the considered optimum conditions were calculated 0.10 kg/m³ and 0.03 kg/m³, respectively ($\Delta(\%)_{\text{Fe}} = 110\%$, $\Delta(\%)_{\text{Al}} = 116\%$). Kobya et al. [38] found that the Faradic yield percent Δ (%) for their electrodes were varied 106–116%. Cost due to real electrode consumption (anode dissolution as well as anode and cathode pitting corrosion) in the optimum condition is

calculated based on the given electrode consumption and reported electrode prices in Table 2, 0.004 €/m³ and 0.011 €/m³ for anode and cathode, respectively. Therefore the operating cost is about 0.029 €/m³. At the present Iran wastewater company (IWWC) produced fresh water at the price of 0.28 €/m³. Phalakornkule et al. [2] reported that the operating cost of the dye removal using EC process was lower than 0.12 €/m³.

The specific electrical energy consumption (SEEC) can be expressed as a function of electrodes weight loss throughout EC process in kWh/(kg Fe or Al electrodes) [4, 41]:

$$\text{SEEC} = \frac{z \times F \times \epsilon}{3600 \times M \times \Delta} \quad (18)$$

where z , F , M and ϵ were identified in Eqs. (1) and (3), respectively. Also Δ , current efficiency or Faradic yield, was calculated by Eq. (17). In Table 1, SEEC was calculated for four conditions of SPC electrocoagulation and compared with optimum condition of DC electrocoagulation of AB113 dye removal. The results show that SPC electrocoagulation can effectively reduce SEEC than DC electrocoagulation to a very low level. The results are in agreement with the subsequent research [41].

3.6. Characterization of dried sludge and floated flocs powder

3.6.1. FTIR analysis

Fig. 8 shows the FTIR spectrum of the dried sludge/floc obtained in the AB113 dye removal by EC process. A strong and intense band at 3424.73 cm⁻¹ can be assign to OH-stretching vibration of hydroxyl group of iron hydroxide/oxy-hydroxide [5]. The sharp peak at 2923.35 cm⁻¹ is due to C-H stretching mode of saturated hydrocarbons (C-C band) connected to aromatic cleavage in the dried sludge/floc residue [42]. A sharp and broad peak at 1630.81 cm⁻¹ can be assign OH-bending and confirms the presence of iron oxy-hydroxide [5,43]. In the wavelengths of 1385.48 and 1171.5 cm⁻¹ appearance of two weak peaks are due to respectively, S-O stretching vibration of SO₃⁻ group and aromatic ring stretching of AB113 dye molecule [5,44].

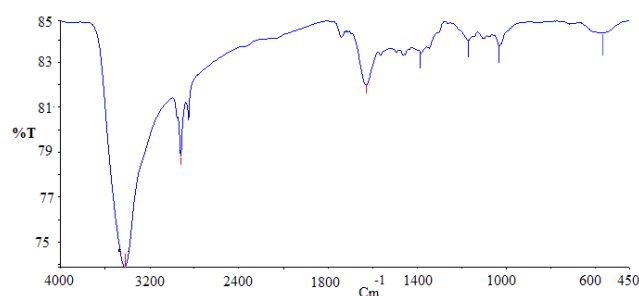


Fig. 8. FTIR spectrum of the dried sludge/floc produced from AB113 dye removal by the EC process (square pulse current type (SPC)).

Also other weak peaks at 1034.33 and 1400 cm^{-1} are due to OH-bending for Al–OH vibrations [18,45–46]. A broad and weak band with low intensity at 596 cm^{-1} is due to Fe–O/ Fe_2O_3 in amorphous ferrihydrite [47–50]. It is interesting to note that the peaks (at 1596 and 1106 cm^{-1}) which are due to azo band are absent in the dye FTIR spectrum [5].

3.6.2. Scanning electron microscopy (SEM)

The morphology image of dried sludge and floated flocs formed during the removal of AB113 dye by electrocoagulation is shown in Fig. 9. In this SEM image, the presence of pseudo sphere nanoparticles within the size of 70–100 nm is observed.

3.6.3. Energy dispersive analysis by X-rays (EDAX)

In order to know the constituents of the dried sludge/floc produced in AB113 dye removal by EC process, elemental analysis was performed with the EDAX. The presence of Fe, O, Na, Cl, Al, Mg, Cr and S in the spectrum are shown in Fig. 10, respectively at 7.0, 22.0, 41, 25.0, 2.0, 0.2, 0.4 and 2.4 (atomic%). Two main EDAX peaks are attributed to the NaCl supporting electrolyte. Due to the presence of hydroxyl ions, the cathodic (Al) dissolution occurs because the generated by the water reduction can attack and destroy the Al electrode and consequently aluminum peak appears in EDAX pattern. Similar results are reported by other researchers [43,51]. The presence of Mg and Cr atoms are due to iron or aluminum electrodes impurities (Fe/Al alloy, electrodes) and the S atom is from of AB113 dye molecule constituents. However the negligible residual concentration of soluble metals (Fe, Al, Mg and Cr) in the EC supernatant sample are measured and analyzed by atomic absorption.

3.6.4 XRD analysis

In this investigation the obtained dried sludge and floated flocs powder after AB113 dye removal electrocoagulation was characterized by XRD (Philips/PW1800-Netherlands). XRD spectrum was performed using Cu–K α radiation, voltage of 40 kV and amperage 30 mA, step scanning $2\theta = 2\text{--}90^\circ$ and $\lambda = 0.1542 \text{ nm}$ [24] represented in Fig. 11. It is evident that there are 2 main shallow peaks centered at 28° and 64.1° of 2θ , indicating amorphous or

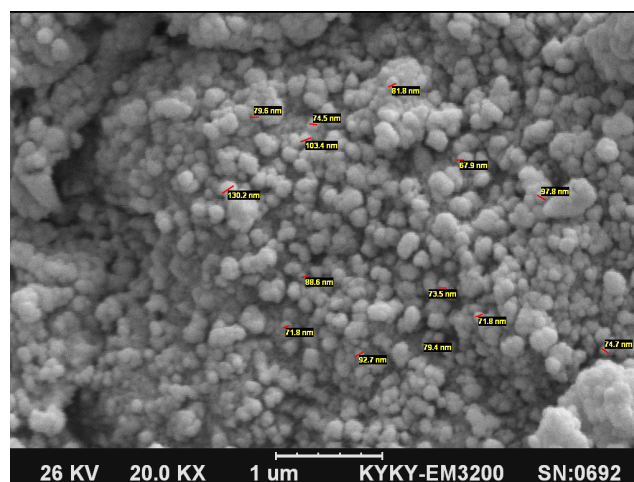


Fig. 9. SEM image of dried sludge/floc formation during the removal of AB113 dye by EC process (square pulse current type (SPC)).

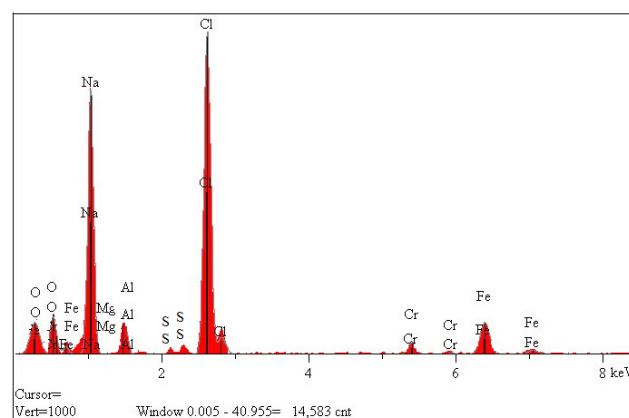


Fig. 10. EDAX spectrum of the dried sludge/floc produced on AB113 dye removal in the electrocoagulation process (at the optimum condition; initial AB113 dye concentration 500 mg/L, CD 70A/m 2 , initial pH 5, conductivity 1.7 mS/cm, (square pulse current type (SPC))).

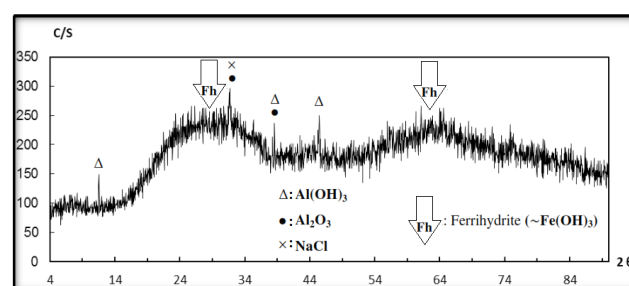


Fig. 11. XRD spectrum of the dried sludge and floated flocs (sludge/floc) powder produced on AB113 dye removal in the electrocoagulation process (at the optimum condition; initial AB113 dye concentration 500 mg/L, CD 70A/m 2 , initial pH 5, conductivity 1.7 mS/cm, square pulse current type (SPC)).

poorly crystalline phase 2-line ferrihydrite (PDF 29-0712 data base) [49,51–55]. In the literature some researchers predicted that Ferrihydrite as $\text{Fe}(\text{OH})_3$ [55,56]. The peaks at $2\theta = 11.55, 38.55$ and 45.44° which are interpreted as $\text{Al}(\text{OH})_3$ [56–58] whereas, the peaks at $2\theta = 31.68$ and 38.55° are due to the Al_2O_3 [56] also the presence of crystalline Hallite (NaCl) was identified [59].

The SEM, FTIR, EDAX and XRD results confirms the precipitation of nano particles of iron and aluminum hydroxid /oxy-hydroxid ($\text{Fe}(\text{OH})_3, \text{Al}(\text{OH})_3$) [50,54–58].

3.7. Kinetics of electrocoagulation

In the dye removal by the EC process the dissolved dye is practically adsorbed on the surface of the produced sludge/floc [5]: at the first stage, flocs of the metallic fine particles are produced during the oxidation at the anode, by electrode dissolving, and then hydrolysis to form flocs of metallic hydroxide. In the second stages the adsorption and coagulation between dye molecule and metallic hydroxides occur by electrostatic attraction or physico/chemical complexation [6]. Finally the generated insoluble sludge/ floc are precipitated or floated (Fig. 2). However the weight loss of electrodes can be obtained either by using Faraday's law (Eq. (1)) or by weighting the electrodes before and after each EC batch. In this study according to the SEM image (Fig. 9), the fundamental role of the adsorption phenomenon in the EC process is indicated by presence of nanoparticles sludge/floc as an efficient adsorbents. Therefore the dye removal can be represented by considering the adsorption results [6] such as evaluating the experimental adsorption capacity, Q_{Exp} (mg/g) (or the amount of dye adsorbed per mass of adsorbent). Q_{Exp} can be evaluated by using the following material balance equation:

$$Q_{\text{exp}} = \frac{C_0 - C_e}{M} \cdot V \quad (19)$$

where C_0 and C_e (mg/L) are the dye concentrations at initial and at equilibrium time t , respectively, V is the initial volume of the dye solution (L), M is the adsorbent mass (g) in electrocoagulation process and M can be interpreted as weight loss (g) of the electrode by electrode dissolution.

For studying the rate of dye adsorption by insoluble iron and aluminum hydroxide nanosludge/floc in the EC process, two of fundamental and well known rate equations namely pseudo-first-order and pseudo-second-order rate equations were examined. The pseudo-first-order rate equation can be represented as [61]:

$$Q_t = Q_e(1 - \exp^{-k_1 t}) \quad (20)$$

where K_1 (1/min) is the adsorption rate constant for pseudo-first-order rate equation, Q_t (mg/g) and Q_e (mg/g) are the adsorption capacity at time t and at equilibrium time, respectively.

The pseudo-second-order rate equation is given as [62]:

$$Q_t = \frac{K_2 Q_e^2 t}{1 + K_2 Q_e t} \quad (21)$$

where (g/(mg·min)) is the adsorption rate constant for pseudo-second-order rate equation.

The non-linear regression has been considered as a suitable criterion for investigating the correspondence of curve fitting between experimental and calculated results. Therefore in order to judge the acceptability of the rate equations to treat the experimental results, the average relative error percent (A.R. Error %) was evaluated by using the following equation:

$$A.R. Error \% = \frac{100}{n} \sum_{i=1}^n \left| \frac{Q_{\text{exp}} - Q_{\text{Cal}}}{Q_{\text{exp}}} \right| \quad (22)$$

where Q_{Exp} and Q_{Cal} (mg/g) are the experimental and calculated (by applying the rate equation) adsorption capacities, respectively. The smaller value of A.R. Error % indicates a proper curve fitting and acceptability of the corresponding equation [63].

Also the non-linear chi-square test χ^2 is defined as [64]:

$$\chi^2 = \sum_{i=1}^n \frac{(Q_{\text{exp}} - Q_{\text{Cal}})^2}{Q_{\text{exp}}} \quad (23)$$

which can be used for the curve fitting tests. This test is necessary for evaluating the best curve fit to the adsorption data. When the calculated and experimental adsorption capacities are similar, the small value represents the correlation between experimental and calculated data. However a large value of indicates a difference and no correlation.

The adsorption curves treated by Eqs. (20) and (21) are depicted in Fig. 12. The rate parameters are represented in Table 2. According to the results in Fig. 12 and Table 3, it can be seen that the adsorption rates of AB113 dye in the EC process is well described by the pseudo-second-order adsorption rate equation (with lower A.R. Error % (2.2) and lower value of 14.6. Other researchers are obtained similar results [6].

3.8. Adsorption isotherm study

In this section we examine which adsorption isotherm equation is more appropriate to treat the experimental

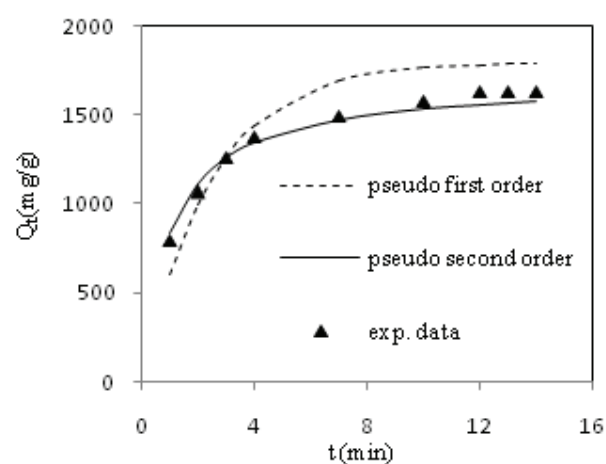


Fig. 12. Rate of adsorption of the AB113 dye in the EC process (at the optimum condition; AB113 dye concentration of 500 mg/L, CD 70A/m², initial pH 5, conductivity 1.7 mS/cm).

Table 3
Kinetic parameters for the removal of AB113 (500 mg/L) during EC process, $Q_{eExp} = 1636$ (mg/L)

Rate equation	Parameters	Value	A.R. Error %	
Pseudo-first-order	K_1 (1/min)	0.405	147.1	9.8
	Q_e (mg/L)	1800.0		
Pseudo-second-order	K_2 (g/(mg·min))	0.00057	14.6	2.2
	Q_e (mg/L)	1696		

data, as obtained in this work for the dye removal by the electrocoagulation. The common adsorption isotherm equations are those of Langmuir, Freundlich, Sips and Temkin [65–73]:

The Langmuir isotherm equation is in the following form [66–68]:

$$Q = \frac{Q_0 b C_e}{1 + b C_e} \quad (24)$$

where b (L/mg) is the Langmuir adsorption binding constant and Q_0 (mg/g) is the maximum adsorption capacity. The adsorption capacity Q (mg/g) is calculated by using the measured residual dye concentration C_e (mg/g) at equilibrium.

The Freundlich adsorption isotherm is [69]:

$$Q = K_F C_e^{1/n} \quad (25)$$

where K_F ((mg/g) (mg/L)^{-1/n}) is the Freundlich constant and n refers to the adsorption intensity. If $1 < n < 10$ the adsorption would be considered is favorable [69].

The Sips isotherm equation is represented as [70]:

$$Q = \frac{K_S C_e^{\beta_S}}{1 + a_S C_e^{\beta_S}} \quad (26)$$

Sips isotherm is generally used for treating the heterogeneous adsorption. There are two limiting states for application of the Sips isotherm; at low concentrations of the adsorbate the Sips model restricts to the Freundlich model; whereas at high concentrations it breaks to the Langmuir model. In this three parameters equation the important experimental conditions (such as pH, initial dye concentration and temperature) effects on the values of operating parameters [71].

In Eq. (26) the exponent, β_S , is the dimensionless dissociation parameter (for $\beta_S = 1$ the Sips isotherm breaks to the Langmuir isotherm), K_S ($L^{\beta_S} \text{ mg}^{1-\beta_S} / \text{g}$) is the maximum adsorption capacity and a_S ($L^{\beta_S} / \text{mg}^{\beta_S}$) is the adsorption constant.

The Temkin isotherm equation is in the following form [72–73]:

$$Q = B_T \ln A_T + B_T \ln C_e \quad (27)$$

where B_T (mg/g) is a function of heat of adsorption and (L/mg) is related to adsorbent–adsorbate interactions.

The adsorption data were treated by the Langmuir, Freundlich, Sips and Temkin isotherm equations [Eqs. (24)–

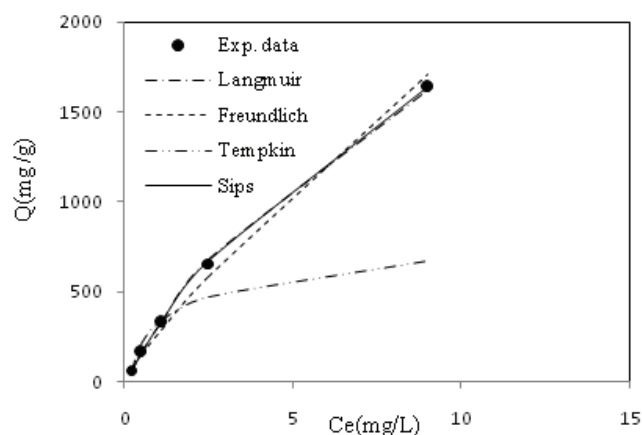


Fig. 13. The AB113 dye removal results treated by various adsorption isotherm equations (at the optimum condition; initial AB113 dye concentration 500 mg/L, CD 70A/m², initial pH 5, conductivity 1.7 mS/cm, equilibrium time 12 min, DC current).

Table 4
Isotherm parameters of AB113 adsorption by sludge/floc nanoparticles produced during EC process

Isotherm models	Parameters	Value	A.R. Error %	
Sips	K_S ($L^{\beta_S} \text{ mg}^{1-\beta_S} / \text{g}$)	328.1	0.37	1.0
	a_S ($L^{\beta_S} / \text{mg}^{\beta_S}$)	0.08		
	β_S	0.98		
Langmuir	b (L/mg)	0.096	0.87	1.6
	Q_0 (mg/L)	3500		
Freundlich	K_F ((mg/g) (mg/L) ^{-1/n})	270.4	17.43	8.0
	n	1.19		
Temkin	A_T (L/mg)	7.55	632	23
	B_T (mg/g)	160.0		

(27)]. The results are represented in Fig. 13 and Table 4. The results indicate that the Sips isotherm effectively fits the data as obtained for adsorption of the dye onto the nanoparticles of sludge/floc produced in the EC process. The isotherm constants parameters are reported in Table 4. The low value of A.R. Error % = 1 and low value of non-linear chi-square test parameter $\chi^2 = 0.37$ for the Sips equation indicates that the Sips isotherm equation can properly describe the adsorption results. Unfortunately, no reports were found for treating the dye electrocoagulation results by isotherm adsorption models to make a significant comparison.

4. Conclusion

Electrocoagulation (EC) process as an efficient method has been used for uptake of acid blue 113 (AB113) dye as a hazardous pollutant effluent of the dye industries. The operating parameters of EC process by application of iron(anode)/aluminum (cathode) as the electrodes were

optimized by considering the effect of their variation such that; the initial dye concentration (20–500 mg/L), initial pH (1–9) and current density (20–120 Am⁻²). The other effective parameters which were examined to investigate their effect on the dye removal included the electrolyte concentration (0.2–1 g/L), water reclamation yield, type of current (direct and square pulse), electrical energy and specific electrical energy consumption (SEEC). The optimum condition for SPC electrocoagulation: initial pH 5, initial dye concentration 500 mg/L, volume of wastewater 700 mL, current density (CD) 70 A/m², conductivity 1.7 mS/cm, electrolyte concentration 0.6 g/L, electrical energy 1.2 kWh/m³ of the solution, SEEC 0.1 kWh/kg Fe, and maximum dye uptake (%) 99.66%, maximum COD removal (%) 94%, maximum water reclamation yield (0.95 m³ of clear supernatant after removal/m³ of the solution before removal, square pulse current (3 min off / 3 min on) and as a result the equilibrium time reduces from 12 min (in DC electrocoagulation) to 6 min which indicates less energy consumption. SEEC in optimized SPC electrocoagulation is significantly lower than optimized DC electrocoagulation. The dried sludge/floc was characterized by SEM, EDAX, XRD, and FTIR. Characterization analyses were demonstrated that the sludge/floc is in the form of ferrihydrite (~Fe(OH)₃) and Al(OH)₃, as a superior adsorbents enhanced the adsorption of AB113 dye molecule in the electrocoagulation process. The dye adsorption results were treated by several adsorption isotherms equations and it was found that the Sips isotherm equation indicated the best fit to the obtained results. Also among the rate equations, it was found that the pseudo-second-order rate equation properly expressed the rate of the dye adsorption. The results demonstrated that by imposing the square pulse current EC; the water reclamation yield and energy economization were enhanced more than by the direct current EC. The SEM analysis showed that the obtained sludge/floc were in the form of nano-pseudo sphere particles.

References

- [1] M. Kobya, O.T. Can, M. Bayramoglu, Treatment of textile wastewaters by electrocoagulation using iron and aluminum electrodes, *J. Hazard. Mater.*, 100 (2003) 163–178.
- [2] C. Phalakornkule, P. Sukkasem, C. Mutchimsattha, Hydrogen recovery from the electrocoagulation treatment of dye-containing wastewater, *Int. J. Hydrogen Energy*, 35(20) (2010) 10934–10943.
- [3] O.T. Can, M. Bayramoglu, M. Kobya, Decolorization of reactive dye solutions by electrocoagulation using aluminum electrodes, *Ind. Chem. Res.*, 42 (2003) 3391–3396.
- [4] N. Daneshvar, A.R. Khataee, A.R. Amani Ghadim, M.H. Rasoulifard, Decolorization of C.I. Acid Yellow 23 solution by electrocoagulation process: Investigation of operational parameters and evaluation of specific electrical energy consumption (SEEC), *J. Hazard. Mater.*, 148 (2007) 566–572.
- [5] M. Saravanan, N.P. Sambhamurthy, M. Sivarajan, Treatment of acid blue 113 dye solution using iron electrocoagulation, *Clean – Soil, Air, Water*, 38 (2010) 565–571.
- [6] K. Chithra, N. Balasubramanian, Modeling electrocoagulation through adsorption kinetics, *J. Model. Simulat. Sys.*, 1 (2010) 124–130.
- [7] E. Keshmirizadeh, S. Yousefi, M.K. Rofouei, An investigation on the new operational parameter effective in Cr (VI) removal efficiency: A study on electrocoagulation by alternating pulse current, *J. Hazard. Mater.*, 190 (2011) 119–124.
- [8] E. Brillas, C.A. Martínez-Huitle, Decontamination of wastewaters containing synthetic organic dyes by electrochemical methods, An updated review, *Appl. Catalysis B: Environment.*, 166–167 (2014) 603–643.
- [9] M. Zaied, N. Bellakhal, Electrocoagulation treatment of black liquor from paper industry, *J. Hazard. Mater.*, 163 (2009) 995–1000.
- [10] K. Thirugnanasambandham, V. Sivakumar, J. Prakash Maran, Optimization of process parameters in electrocoagulation treating chicken industry wastewater to recover hydrogen gas with pollutant reduction, *Renew. Energy*, 80 (2015) 101–108.
- [11] M. Kobya, H. Hiz, E. Senturk, C. Aydiner, E. Demirbas, Treatment of potato chips manufacturing wastewater by electrocoagulation, *Desalination*, 190 (2006) 201–211.
- [12] K. Bensadok, N. El Hanafi, F. Lapique, Electrochemical treatment of dairy effluent using combined Al and Ti/Pt electrodes system, *Desalination*, 280 (2011) 244–251.
- [13] X. Chen, G. Chen, P.L. Yue, Separation of pollutants from restaurant wastewater by electrocoagulation, *Sep. Purif. Technol.*, 19 (2000) 65–76.
- [14] S. Gao, M. Du, J. Tian, J. Yang, F. Ma, J. Nan, Effects of chloride ions on electrocoagulation flotation process with aluminum electrodes for algae removal, *J. Hazard. Mater.*, 182 (2010) 827–834.
- [15] N. Adhoum, L. Monser, N. Bellakhal, J. Eddine Belgaied, Treatment of electroplating wastewater containing Cu²⁺, Zn²⁺ and Cr(VI) by electrocoagulation, *J. Hazard. Mater.*, B 112 (2004) 207–213.
- [16] M. Ren, Y. Song, Sh. Xiao, P. Zeng, J. Peng, Treatment of berberine hydrochloride wastewater by using pulse electrocoagulation process with Fe electrode, *Chem. Eng. J.*, 169 (2011) 84–90.
- [17] J. Jiang, N. Graham, C. André, G.H. Kelsall, N. Brandon, Laboratory study of electro-coagulation–flotation for water treatment, *Water Res.*, 36 (2002) 4064–4074.
- [18] Y.A.M. Mollah, P. Morkovsky, J.A.G. Gomes, M. Kesmez, J. Parga, D.L. Cocke, Fundamentals, present and future perspectives of electrocoagulation, *J. Hazard. Mater.*, 114 (2004) 199–210.
- [19] P.K. Holt, G.W. Barton, M. Wark, C.A. Mitchell, A quantitative comparison between chemical dosing and electrocoagulation, *Colloids Surf. A Physico chem. Eng. Aspects*, 211 (2002) 233–248.
- [20] J.S. Do, M.L. Chen, De colorization of dye containing solutions by electrocoagulation, *J. Appl. Electrochem.*, 24 (1994) 785–790.
- [21] N.K. Khosla, S. Venkatachalam, P. Somasundaran, Pulsed electrogeneration of bubbles for electroflotation, *J. Appl. Electrochem.*, 21 (1991) 986–990.
- [22] J. Duan, J. Gregory, Coagulation by hydrolysing metal salts. *Adv. Colloid Interface*, 100 (2003) 475–502.
- [23] APHA-AWWA, WPCF, Standard Methods for the Examination of Water and Wastewater, twenty-first Ed.; American Public Health Association, Washington, DC, 2005.
- [24] E. Moaveni, E. Keshmirizadeh, H. Modarress, Removal of acid red 151 dye from water by iron-impregnated heat treated egg shell bio-adsorbent, *Desal. Water Treat.*, 67 (2017) 309–317.
- [25] J. Basiri Parsa, H. Rezaei Vahidian, A.I. R. Soleymani, M. Abbasi, Removal of Acid Brown 14 in aqueous media by electrocoagulation: optimization parameters and minimizing of energy consumption. *Desalination*, 278 (2011) 295–302.
- [26] C. Barrera-Díaz, F. Ureña-Núñez, E. Campos, A combined electrochemical-irradiation treatment of highly colored and polluted industrial wastewater., *Radiat. Phys. Chem.*, 67 (2003) 657–663.
- [27] T.S. Anantha Singh, S. Thanga Ramesh, An experimental study of CI Reactive Blue 25 removal from aqueous solution by electrocoagulation using aluminum sacrificial electrode: kinetics and influence of parameters on electrocoagulation performance, *Desal. Water Treat.*, 52 (2014) 2634–2642.
- [28] Y. Yavuz, E. Ocal, A. Koparala, U.B. Ogutverena, Treatment of dairy industry wastewater by EC and EF processes using hybrid Fe–Al plate Electrodes, *J. Chem. Technol. Biotechnol.*, 86 (2011) 964–969.

- [29] J.B. Lumsden, P.J. Stocker, S.C. Tsai, The composition and morphology of pits formed on iron in an inhibited chloride solution, *Appl. Surf. Sci.*, 7 (1981) 347–354.
- [30] M.G. Arroyo, V. Pérez-Herranz, M.T. Montañés, J. García-Antón, J.L. Guiñón, Effect of pH and chloride concentration on the removal of hexavalent chromium in a batch electrocoagulation reactor, *J. Hazard. Mater.*, 169 (2009) 1127–1133.
- [31] G. Moussavi, R. Khosravi, M. Farzadkia, Removal of petroleum hydrocarbons from contaminated groundwater using an electrocoagulation process: Batch and continuous experiments, *Desalination*, 278 (2011) 288–294.
- [32] C.A. Martínez-Huitle, E. Brillas, Decontamination of wastewaters containing synthetic organic dyes by electrochemical methods: a general review, *Appl. Catal. B-Environ.*, 87 (2009) 105–145.
- [33] R. William Puls, Capstone report on the application, monitoring, and performance of permeable reactive barriers for groundwater remediation, Volume 1, EPA/600/R-03/045a, (2003).
- [34] P.N. Johnson, A. Amirtharajah, Ferric Chloride and Alum as Single and Dual Coagulants, *J. AWWA*, 75 (1983) 232–239.
- [35] W.J. Weber, *Physico Chemical Processes for Water Quality Control*, John Wiley and Sons, Inc., New York, (1972).
- [36] G.E. Findlay, L.F. Darryl, Electrolytic treatment of an industrial wastewater from a hosiery plant, *Water Environ. Res.*, 78 (2006) 435–441.
- [37] A. Karkhaneh, E. Keshmirizadeh, Removal of crude oil from oily artificial wastewater by using pulse electrochemical treatment, *J. Appl. Chem. Res.*, 9 (Special issue) (2015) 55–65.
- [38] M. Kobya, U. Gebologlu, F. Ulu, S. Oncel, E. Demirbas, Removal of arsenic from drinking water by the electrocoagulation using Fe and Al Electrodes, *Electrochim. Acta*, 56(14) (2011) 5060–5070.
- [39] M. Liu, Y. Jin, C. Zhang, C. Leygraf, L. Wen, Density-functional theory investigation of Al pitting corrosion in electrolyte containing chloride ions, *Appl. Surf. Sci.*, 357B (2015) 2028–2038.
- [40] P. Marcus, *Corrosion Mechanism in Theory and Practice*, Second Ed., Marcel Dekker, New York, 2002.
- [41] D. Ghosh, H. Solanki, M.K. Purkait, Removal of Fe(II) from tap water by electrocoagulation technique, *J. Hazard. Mater.*, 155 (2008) 135–143.
- [42] D. Pavia, G. Lampman, G. Kriz, J. Vyvyan, *Introduction to Spectroscopy*, Cengage Learning, (2008).
- [43] S. Vasudevan, A. Margrat Sheela, J. Lakshmia, G. Sozhan, Optimization of the process parameters for the removal of boron from drinking water by electrocoagulation—a clean technology, *J. Chem. Technol. Biotechnol.*, 85 (2010) 926–933.
- [44] M.V. Anand, V.C. Srivastava, S. Singh, R. Bhatnagar, I.D. Mall, Electrochemical treatment of alkali decrement wastewater containing terephthalic acid using iron electrodes, *J. Taiwan Inst. Chem. Eng.*, 45 (2014) 908–913.
- [45] K. Vinodgopal, D.E. Wynkop, P.V. Kamat, Environmental photochemistry on semiconductor surfaces. A photosensitization approach for the degradation of a textile Azo Dye, Acid Orange 7, *Environ. Sci. Technol.*, 30 (1996) 1660–1666.
- [46] H. Kodoma, M. Schnitzer, Effect of fulvic acid on the crystallization of aluminum hydroxides, *Geoderma*, 24 (1980) 195–205.
- [47] A. Nezamzadeh-Ejchieh, A. Shirzadi, Enhancement of the photocatalytic activity of Ferrous Oxide by doping onto the nano-clinoptilolite particles towards photodegradation of tetracycline, *Chemosphere*, 107 (2014) 136–144.
- [48] A. Boudjema, A. Rebahi, B. Terfassa, R. Chebout, T. Mokrani, K. Bachari, N.J. Coville, Fe₂O₃/carbon spheres for efficient photo-catalytic hydrogen production from water and under visible light irradiation, *Solar Energy Mat. Solar Cell.*, 140 (2015) 405–411.
- [49] D. Xu, X. Lai, W. Guo, P. Dai, Microwave-assisted catalytic degradation of methyl orange in aqueous solution by ferrihydrite/maghemite nanoparticles, *J. Water Proc. Eng.*, 16 (2017) 270–276.
- [50] E. Chmielewska, W. Tylus, M. Drábik, J. Majzlan, L. Čaplovič, Structure investigation of nano-FeO(OH) modified clinoptilolite tuff for antimony removal, *Micropor. Mesopor. Mat.*, 248 (2017) 222–233.
- [51] T. Picard, G. Cathalifaud-Feuillade, M. Mazet, C. Vandensteendam, Cathodic dissolution in the electrocoagulation process using aluminium electrodes, *J. Environ Monit.*, 2 (2000) 77–80.
- [52] S. Skov Nielsen, P. Kjeldsen, H. Christian Bruun Hansen, R. Jakobsen, Transformation of natural ferrihydrite aged in situ in As, Cr and Cu contaminated soil studied by reduction kinetics, *Appl. Geochem.*, 51 (2014) 293–302.
- [53] A. Al Mamun, M. Morita, M. Matsuoka, Ch. Tokoro, Sorption mechanisms of chromate with coprecipitated ferrihydrite in aqueous solution, *J. Hazard. Mater.*, 334 (2017) 142–149.
- [54] Ch. Poggenburg, R. Mikutta, M. Sander, A. Schippers, G. Guggenberger, Microbial reduction of ferrihydrite-organic matter coprecipitates by *Shewanella putrefaciens* and *Geobacter metallireducens* in comparison to mediated electrochemical reduction, *Chem. Geol.*, 447 (2016) 133–147.
- [55] J. Majzlan, A. Navrotsky, U. Schwertmann, Thermodynamics of iron oxides: part III. Enthalpies of formation and stability of ferrihydrite (–Fe(OH)₃), schwertmannite (–FeO(OH)₃/4(SO₄)₁/8), and ε-Fe₂O₃, *Geochim. Cosmochim. Acta.*, 68 (2004) 1049–1059.
- [56] J.M. Zachara, R. Kukkadapu, J.K. Fredrickson, Y.A. Gorby, S.C. Smith, Biomining of poorly crystalline Fe (III) oxides by dissimilatory metal reducing bacteria (DMRB), *Geomicrobiol. J.*, 19 (2002) 179–207.
- [57] P. Aswathy, R. Gandhimathi, S.T. Ramesh, P.V. Nidheesh, Removal of organics from bilge water by batch electrocoagulation process, *Sep. Purif. Technol.*, 159 (2016) 108–115.
- [58] K. Govindan, M. Raja, S. Uma Maheshwari, M. Noel, Y. Oren, Comparison and understanding of fluoride removal mechanism in Ca²⁺, Mg²⁺ and Al³⁺ ion assisted electrocoagulation process using Fe and Al electrodes, *J. Environ. Chem. Eng.*, 3 (2015) 1784–1793.
- [59] K. Govindan, Y. Oren, M. Noel, Effect of dye molecules and electrode material on the settling behavior of flocs in an electrocoagulation induced settling tank reactor (EISTR), *Sep. Purif. Technol.*, 133 (2014) 396–406.
- [60] U. Tezcan Un, S. Eroglu Onpeker, E. Ozel, The treatment of chromium containing wastewater using electrocoagulation and the production of ceramic pigments from the resulting sludge, *J. Environ. Manage.*, 200 (2017) 196–203.
- [61] S. Lagergren, About the theory of so called adsorption of soluble substances, *Ksver. Vetenskapsakad. Handl.*, 24 (1898) 1–6.
- [62] Y.S. Ho, G. McKay, Pseudo-second order model for sorption processes, *Process Biochem.*, 34 (1999) 451–465.
- [63] A. Kapoor, R.T. Yang, Correlation of equilibrium adsorption data of condensable vapours on porous adsorbents, *Gas Sep. Purif.*, 3(1989) 187–192.
- [64] B. Boulinguez, P. Le Cloirec, D. Wolbert, Revisiting the determination of Langmuir parameters application to tetrahydrothiophene adsorption onto activated carbon, *Langmuir*, 24 (2008) 6420–6424.
- [65] Y. A. Ouaisa, M. Chabani, A. Amrane, A. Bensmaili, Removal of tetracycline by electrocoagulation: Kinetic and isotherm modeling through adsorption, *J. Environ. Chem. Eng.*, 2 (2014) 177–184.
- [66] A.W. Adamson, *Physical chemistry of surfaces*. 6th Ed., John Wiley & Sons, Inc, (1997).
- [67] I. Langmuir, The constitution and fundamental properties of solids and liquids, Part I, Solids, *J. Am. Chem. Soc.*, 38 (1916) 2221–2295.
- [68] I. Langmuir, The Adsorption of Gases on Plane Surfaces of Glass, Mica, and Platinum, *J.A. Chem. Soc.*, 40 (1918) 1361–1403.
- [69] H.M.F. Freundlich, Über die adsorption in lösungen, *Z. Phys. Chem. (Leipzig)*, 57A (1906) 385–470.

- [70] R. Sips, Combined form of Langmuir and Freundlich equations, *J. Chem. Phys.*, 16 (1948) 490–495.
- [71] A.B. Pérez-Marín, V. Meseguer Zapata, J.F. Ortuno, M. Aguilar, J. Sáez, M. Llorens, Removal of cadmium from aqueous solutions by adsorption onto orange waste, *J. Hazard. Mater.*, 139 (2007) 122–131.
- [72] M.I. Tempkin, V. Pyzhev, Kinetics of ammonia synthesis on promoted iron catalyst, *Acta Phys. Chim. USSR*, 12 (1940) 327–356.
- [73] C. Aharoni, M. Ungarish, Kinetics of activated chemisorptions, Part 2, Theoretical models, *J. Chem. Soc. Faraday Trans.*, 73 (1977) 456–464.